

# Cartesian Impedance Control of Redundant Robots: Recent Results with the DLR-Light-Weight-Arms

Alin Albu-Schäffer, Christian Ott, Udo Frese and Gerd Hirzinger

DLR - German Aerospace Center  
Institute of Robotics and Mechatronics  
*alin.albu-schaeffer@dlr.de, christian.ott@dlr.de*

**Abstract**— This paper addresses the problem of impedance control for flexible joint robots based on a singular perturbation approach. Some aspects of the impedance controller, which turned out to be of high practical relevance during applications are then addressed, such as the implementation of nullspace stiffness for redundant manipulators, the avoiding of mass matrix decoupling and the related design of the desired damping matrix. Finally, the proposed methods are validated through measurements on the DLR robot.

## I. INTRODUCTION

The topic of impedance control is a traditional one in robotics. It provides a very suitable framework for controlling robots in contact with an unknown environment [5]. However, the focus on this field is renewed because of applications such as force feedback, or service and medical robotics, where safety of interaction is crucial. Those applications require also highly light-weight arms, which have minimal impact inertia and can be mounted on mobile systems. Because of the inherent flexibility of the light-weight structures, it becomes necessary to bring together the control field of flexible joint robots with that of compliant control. In [1], various Cartesian compliant control strategies (admittance, impedance and stiffness control) were compared and implemented on the DLR light-weight robots. Because of the rather slow Cartesian sampling rate (6ms), classical impedance control had the poorest performance. This changed significantly by increasing the sampling rate to 1ms, enabling the implementation of high quality impedance control. The recent results with the Cartesian impedance controller are the topics of this paper.

The singular perturbation theory is used to extend existing impedance control methods from the rigid body robot case to the flexible joint structure. This simple, but efficient method in case of robots with moderate elasticity uses a fast joint level torque control loop, which is receiving its desired torque from a classical Cartesian impedance controller. The DLR 7DOF light-weight arms (Fig. 1) with integrated joint torque sensors are very well suited for this kind of control algorithms [4]. The paper discusses several methods of providing a nullspace stiffness for the redundant manipulator in addition to a Cartesian stiffness. The difference between the methods is illustrated with



Fig. 1. DLR light-weight robot, generation II, using impedance control in a table wiping application.

measurements. Another practically important aspect was the design of the desired damping matrix in the case that the Cartesian mass matrix is not explicitly decoupled by the controller. Two different approaches to this problem are presented and were verified in experiments.

## II. CONTROL OF THE FLEXIBLE JOINT MODEL

In this paper a model of a robot with  $n$  flexible joints is considered as proposed by Spong [11]:

$$M(\mathbf{q})\ddot{\mathbf{q}} + \mathbf{C}(\mathbf{q}, \dot{\mathbf{q}})\dot{\mathbf{q}} + \mathbf{g}(\mathbf{q}) = \mathbf{K}(\boldsymbol{\theta} - \mathbf{q}) + \boldsymbol{\tau}_{ext}, \quad (1)$$

$$\mathbf{B}\ddot{\boldsymbol{\theta}} + \mathbf{K}(\boldsymbol{\theta} - \mathbf{q}) = \boldsymbol{\tau}_m. \quad (2)$$

Herein  $\mathbf{q} \in \mathbb{R}^n$  and  $\boldsymbol{\theta} \in \mathbb{R}^n$  are the vectors of link positions and the motor positions, respectively.  $M(\mathbf{q})$  denotes the manipulator's mass matrix,  $\mathbf{g}(\mathbf{q})$  the gravity torques and  $\mathbf{C}(\mathbf{q}, \dot{\mathbf{q}})\dot{\mathbf{q}}$  is the vector of Coriolis and centrifugal torques.  $\mathbf{K}$  and  $\mathbf{B}$  are diagonal matrices which contain the joint stiffness and the motor inertias.  $\boldsymbol{\tau} = \mathbf{K}(\boldsymbol{\theta} - \mathbf{q})$  is the vector of joint torques and  $\boldsymbol{\tau}_m$  the motor torque vector which is regarded as the control input. Finally  $\boldsymbol{\tau}_{ext}$  is a vector of external torques, which are exhibited by the manipulator's environment.

One common approach to the control of a flexible joint manipulator is the singular perturbation approach, in

which the flexible joint model is virtually split up into a fast subsystem for the joint torques  $\tau$  and a slow subsystem for the link positions  $q$ . Based on these two subsystems it is possible to design an inner loop controller for the joint torque  $\tau$ , and an outer loop controller for the link position  $q$  separately, without the need to refer to the complete flexible model.

The application of the singular perturbation theory to flexible joint robots has been widely described in the literature and is not in the scope of this paper (see, e.g., [7], [8] for more details). Herein only the resulting controller structure, which will be used in the following sections as a basis for the implementation of different impedance control laws, shall be given briefly.

In [9] it has been shown that, given a desired torque vector  $\tau_d$ , a state feedback controller of the form

$$\tau_m = \tau_d - \mathbf{K}_T(\tau - \tau_d) - \mathbf{K}_S\dot{\tau}, \quad (3)$$

with positiv definite contoller matrices  $\mathbf{K}_T$  and  $\mathbf{K}_S$ , can stabilize the torque dynamics around the equilibrium point  $\tau = \tau_d$ , and leads (under a singular perturbation consideration) to the following link dynamics:

$$\bar{\mathbf{M}}(q)\ddot{q} + \mathbf{C}(q, \dot{q})\dot{q} + \mathbf{g}(q) = \tau_d + \tau_{ext} \quad (4)$$

with  $\bar{\mathbf{M}}(q) = (\mathbf{M}(q) + (\mathbf{I} + \mathbf{K}_T)^{-1}\mathbf{B})$ .

The desired torque vector  $\tau_d$  in (4) can now be used for the realization of a Cartesian impedance controller as will be described in the next section.

### III. CARTESIAN IMPEDANCE CONTROL

Based on the singular perturbation analysis, which was outlined in the last section, a rigid joint robot model of the form (4) may be considered for the design of the Cartesian impedance controller. A detailed study of appropriate Cartesian impedance control laws for nonredundant and redundant rigid robots is given, e.g., in [6].

In the following it is assumed that the manipulator's end-effector position and orientation can be described by a set of local coordinates  $x \in \mathfrak{R}^m$ , and the forward kinematics  $x = f(q)$  is known. The relevant mappings between joint and Cartesian velocities and accelerations can be computed via the Jacobian  $\mathbf{J}(q) = \frac{\partial f(q)}{\partial q}$  as

$$\dot{x} = \mathbf{J}(q)\dot{q}, \quad (5)$$

$$\ddot{x} = \mathbf{J}(q)\ddot{q} + \dot{\mathbf{J}}(q)\dot{q}. \quad (6)$$

Notice that in this paper only the nonsingular case is treated, thus it is assumed that the manipulator's Jacobian  $\mathbf{J}(q)$  has full row rank in the considered region of the workspace. A description of an appropriate singularity treatment can be found in [6].

The deviation of the actual Cartesian position from the desired equilibrium point  $x_d(t)$  is denoted by  $e_x = x - x_d(t)$ . Then the goal for the impedance controller is to

alter the system dynamics (4) such that, in presence of external forces and torques at the end-effector  $\mathbf{F}_{ext} \in \mathfrak{R}^m$ , the closed loop behaviour is given by

$$\Lambda_d\ddot{e}_x + D_d\dot{e}_x + K_d e_x = \mathbf{F}_{ext}, \quad (7)$$

with a desired mass  $\Lambda_d$ , a desired damping  $D_d$  and a desired stiffness matrix  $K_d$ .

In absence of further forces on the arm, the relationship between the external torques  $\tau_{ext}$  and the forces and torques at the end-effector  $\mathbf{F}_{ext}$  is given by:

$$\tau_{ext} = \mathbf{J}(q)^T \mathbf{F}_{ext}. \quad (8)$$

From (6) and (4) one can see that the relationship between the Cartesian accelerations  $\ddot{x}$  and the joint torques  $\tau$  is given by:

$$\ddot{x} - \dot{\mathbf{J}}(q)\dot{q} + \mathbf{J}(q)\bar{\mathbf{M}}(q)^{-1}(\mathbf{C}(q, \dot{q})\dot{q} + \mathbf{g}(q)) = \mathbf{J}(q)\bar{\mathbf{M}}(q)^{-1}(\tau_d + \tau_{ext}). \quad (9)$$

If the desired torque vector  $\tau_d$  is chosen as

$$\tau_d = \mathbf{J}(q)^T \mathbf{F}_\tau + \mathbf{C}(q, \dot{q})\dot{q} + \mathbf{g}(q), \quad (10)$$

with  $\mathbf{F}_\tau \in \mathfrak{R}^m$  as a new control input vector, then the resulting Cartesian behaviour of the robot can be written as:

$$\Lambda(q)(\ddot{x} - \dot{\mathbf{J}}(q)\dot{q}) = \mathbf{F}_\tau + \mathbf{F}_{ext} \quad (11)$$

with

$$\Lambda(q) = (\mathbf{J}(q)\bar{\mathbf{M}}(q)^{-1}\mathbf{J}(q)^T)^{-1} \quad (12)$$

as an equivalent Cartesian mass matrix.

With (11) and (7) it follows that the feedback law

$$\mathbf{F}_\tau = \Lambda(q)\ddot{x}_d - \Lambda(q)\Lambda_d^{-1}(D_d\dot{e}_x + K_d e_x) + (\Lambda(q)\Lambda_d^{-1} - \mathbf{I})\mathbf{F}_{ext} - \Lambda(q)\dot{\mathbf{J}}(q)\dot{q} \quad (13)$$

leads to the desired closed loop behaviour (7).

In [6] it has been shown that, in principle, the same feedback law as described above may also be used in the case of a kinematically redundant manipulator ( $m \neq n$ ). But it is well known that, in the redundant case, also those motions of the joints have to be considered which are embedded in the nullspace of the Jacobian  $\mathbf{J}(q)$  and which do not affect the end-effector position and orientation. Notice that these motions have been eliminated in (9) by the premultiplication with  $\mathbf{J}(q)$ . For a formal analysis of this situation it is necessary to introduce additional nullspace-coordinates  $n$  which, together with the Cartesian coordinates  $x$ , admit a complete description of the robot's dynamics. An interesting set of such nullspace-coordinates with some advantageous properties was introduced by Park in [10].

In order to keep the computational complexity low, in the next section an appropriate extension of the Cartesian impedance controller (10) and (13) is treated, which can be used for the control of the manipulator's nullspace motion without a formal introduction of additional coordinates.

#### IV. NULLSPACE STIFFNESS

In this section it is assumed that the desired nullspace behaviour can be characterized in joint space by a desired positive definite stiffness matrix  $\mathbf{K}_N$  and a positive definite damping matrix  $\mathbf{D}_N$  as well as a desired equilibrium point  $\mathbf{q}_N$ . From these a desired torque  $\boldsymbol{\tau}_{d,N} = -\mathbf{K}_N(\mathbf{q} - \mathbf{q}_N) - \mathbf{D}_N\dot{\mathbf{q}}$  is computed according to a joint level PD-controller. In order to prevent interference with the Cartesian impedance behaviour, this desired torque has to be projected into the manipulator's nullspace by a properly chosen matrix  $\mathbf{N}(\mathbf{q})$ . The desired torque is then composed as

$$\boldsymbol{\tau}_d = \boldsymbol{\tau}_{d,cart} + \mathbf{N}(\mathbf{q})\boldsymbol{\tau}_{d,N} \quad (14)$$

with  $\boldsymbol{\tau}_{d,cart}$  as the impedance controller torque from (10). In the following, three different nullspace projection matrices of different complexities are compared.

##### A. Static Nullspace Projection

Let  $\mathbf{V}(\mathbf{q})$  denote a full rank left annihilator of  $\mathbf{J}^T(\mathbf{q})$ , i.e.,  $\mathbf{V}(\mathbf{q})\mathbf{J}^T(\mathbf{q}) = \mathbf{0}$ . Then a projection matrix of the form

$$\mathbf{N}_1(\mathbf{q}) = \mathbf{V}(\mathbf{q})^T \mathbf{V}(\mathbf{q}) \quad (15)$$

may be used to project the desired torque into the nullspace of the manipulator's Jacobian via  $\boldsymbol{\tau}_0 = \mathbf{N}_1(\mathbf{q})\boldsymbol{\tau}_{d,N}$ .

Notice that in practice the matrix  $\mathbf{V}(\mathbf{q})$  may be computed by a singular value decomposition of the Jacobian. Notice also that, in principle,  $\mathbf{V}(\mathbf{q})$  could also be used for the construction of nullspace coordinates  $\mathbf{n}$ , which were mentioned in the last section, via  $\dot{\mathbf{n}} = \mathbf{V}(\mathbf{q})\dot{\mathbf{q}}$ .

##### B. Dynamically Consistent Projection

It is well known that a static nullspace mapping is not sufficient in order to get a nullspace torque which does not affect the Cartesian behaviour. This can be easily seen by regarding the dynamical equations. A sufficient condition for a nullspace mapping to be consistent with the equations of motion is given by

$$\mathbf{J}(\mathbf{q})\bar{\mathbf{M}}(\mathbf{q})^{-1}\mathbf{N}(\mathbf{q}) = \mathbf{0}, \quad (16)$$

as can be seen from (9). Obviously, this condition can be fulfilled for example with a mapping of the form

$$\mathbf{N}_2(\mathbf{q}) = \bar{\mathbf{M}}(\mathbf{q})\mathbf{V}(\mathbf{q})^T \mathbf{V}(\mathbf{q}) \quad (17)$$

in which the static nullspace projection matrix is premultiplied, and thus scaled, by the manipulator's mass matrix. Another dynamically consistent nullspace mapping, which fits very well in the framework of operational space control, was proposed by Khatib [6]:

$$\mathbf{N}_3(\mathbf{q}) = (\mathbf{I} - \mathbf{J}^T(\mathbf{q})\boldsymbol{\Lambda}(\mathbf{q})\mathbf{J}(\mathbf{q})\bar{\mathbf{M}}^{-1}(\mathbf{q})) . \quad (18)$$

This mapping has the conceptual advantage of being a projection matrix ( $\mathbf{N}_3\mathbf{N}_3 = \mathbf{N}_3$ ), thus avoiding the above mentioned scaling from  $\mathbf{N}_2$ . In order to implement this mapping, the Cartesian mass matrix is needed as well as the inverse of the joint mass matrix. But it is important to notice that these values have to be computed also for the implementation of the general impedance control law in (13).

#### V. AVOIDING THE DECOUPLING OF THE INERTIAL BEHAVIOUR

The decoupling of the inertial behaviour and the command of an arbitrary desired mass matrix in (7) using the controller (13) turns out to be very difficult to realize in practice. Looking at (13), it is clear that the decoupling can not be applied around the robot singularities, since the singularity of  $\mathbf{J}(\mathbf{q})$  implies through (12) that some of the elements of  $\boldsymbol{\Lambda}(\mathbf{q})$  will tend to infinity. This would in turn lead to infinite desired joint torques using (13), (10). But even in regions of the workspace where  $\mathbf{J}(\mathbf{q})$  is well-conditioned, the experimental success was limited in terms of the range of reachable values and of the decoupling accuracy. Possible reasons therefore are in our opinion:

- The influence of joint friction, which cannot be completely eliminated by the joint torque controller and a feed-forward friction compensation.
- The limited accuracy of the dynamical model.
- The additional need to measure the Cartesian force at the end-effector  $\mathbf{F}_{ext}$ , which is in our setup only available with lower sampling rate of 6 ms.

As an alternative to (13), by focusing only on the implementation of Cartesian stiffness and damping, the following simpler control law was preferred:

$$\mathbf{F}_\tau = \boldsymbol{\Lambda}(\mathbf{q})\ddot{\mathbf{x}}_d - \mathbf{D}_d\dot{\mathbf{e}}_x - \mathbf{K}_d\mathbf{e}_x - \bar{\mathbf{C}}(\mathbf{q}, \dot{\mathbf{q}})\dot{\mathbf{e}}_x - \boldsymbol{\Lambda}(\mathbf{q})\dot{\mathbf{J}}(\mathbf{q})\dot{\mathbf{q}} \quad (19)$$

$$\boldsymbol{\tau}_d = \mathbf{J}(\mathbf{q})^T \mathbf{F}_\tau + \mathbf{C}(\mathbf{q}, \dot{\mathbf{q}})\dot{\mathbf{q}} + \mathbf{g}(\mathbf{q}), \quad (20)$$

where  $\bar{\mathbf{C}}(\mathbf{q}, \dot{\mathbf{q}})$  can be an arbitrary matrix, for which the skew symmetry of  $\dot{\boldsymbol{\Lambda}}(\mathbf{q}) - 2\bar{\mathbf{C}}(\mathbf{q}, \dot{\mathbf{q}})$  holds, e.i.  $\bar{\mathbf{C}}(\mathbf{q}, \dot{\mathbf{q}}) = 1/2\dot{\boldsymbol{\Lambda}}(\mathbf{q})$ . This leads to the following closed loop dynamics:

$$\boldsymbol{\Lambda}(\mathbf{q})\ddot{\mathbf{e}}_x + \mathbf{D}_d\dot{\mathbf{e}}_x + \mathbf{K}_d\mathbf{e}_x + \bar{\mathbf{C}}(\mathbf{q}, \dot{\mathbf{q}})\dot{\mathbf{e}}_x = \mathbf{F}_{ext}. \quad (21)$$

Equation (21) represents a passive mapping from the external force  $\mathbf{F}_{ext}$  to the velocity error  $\dot{\mathbf{e}}_x$ , ensuring the stability of the system in free motion and in feedback interconnection with a passive environment.

#### VI. DAMPING DESIGN

While imposing the closed loop dynamics (21) to the robot, the question raises up, how to design the desired damping matrix  $\mathbf{D}_d$  depending on the desired stiffness  $\mathbf{K}_d$  and the actual Cartesian mass matrix of the arm  $\boldsymbol{\Lambda}(\mathbf{q})$ .

What the user may wish to specify for an application, is a well defined damping behaviour in every Cartesian direction (e.g., a critically damped one). It is then obvious that the damping matrix  $D_d$  cannot be constant, but has to be chosen as a function of  $\Lambda(q)$ . In the following, the variation of  $\Lambda(q)$  will be considered slow, so that its derivative can be neglected, reducing (21) in the absence of external forces to

$$\Lambda(q)\ddot{e}_x + D_d\dot{e}_x + K_d e_x = \mathbf{0}. \quad (22)$$

All matrices which will be derived from  $\Lambda(q)$  are assumed to be quasi-static as well.

#### A. Factorization Design

If the eigenvalues of the impedance dynamics should be all real, it can be easily seen that this can be achieved by a damping matrix of the form  $D_d(q) = A(q)K_{d1} + K_{d1}A(q)$ , where  $A(q)$  and  $K_{d1}$  are defined as  $A(q)A(q) = \Lambda(q)$  and  $K_{d1}K_{d1} = K_d$  respectively. (22) can then be factorized as

$$A(q)(A(q)\dot{e}_x + K_{d1}\dot{e}_x) + \quad (23)$$

$$+ K_{d1}(A(q)\dot{e}_x + K_{d1}e_x) = \mathbf{0}. \quad (24)$$

With the substitution  $A(q)\dot{e}_x + K_{d1}e_x = w$ , this leads to the system

$$A(q)\dot{e}_x + K_{d1}e_x = w \quad (25)$$

$$A(q)\dot{w} + K_{d1}w = \mathbf{0}, \quad (26)$$

which has  $n$  pairs of equal, real eigenvalues. An heuristic design approach may then be to choose a general damping design of the form

$$D_d(q) = A(q)D_\xi K_{d1} + K_{d1}D_\xi A(q), \quad (27)$$

where  $D_\xi = \text{diag}\{\xi_i\}$  is a diagonal matrix and  $0 \leq \xi_i \leq 1$  (0 for undamped behaviour and 1 for real eigenvalues). For a wide stiffness range this approach leads indeed to numerical eigenvalues with a damping very close to the desired one.

#### B. Double Diagonalization Design

An more elegant approach to the design of the damping matrix can be developed based on the generalized eigenvalue problem known from matrix algebra [3]:

Given a symmetric positive definite  $n \times n$  matrix  $\Lambda$  and a symmetric  $n \times n$  matrix  $K_d$ , a  $n \times n$  nonsingular matrix  $Q$  can be found, such that  $\Lambda = QQ^T$  and  $K_d = QK_{d0}Q^T$  for some diagonal matrix  $K_{d0}$ .

By choosing the damping matrix as:

$$D_d(q) = 2Q(q)D_\xi K_{d0}^{1/2} Q^T(q), \quad (28)$$

an error dynamics of the form

$$Q(q)Q^T(q)\ddot{e}_x + 2Q(q)D_\xi K_{d0}^{1/2} Q^T(q)\dot{e}_x + \quad (29)$$

$$Q(q)K_{d0}Q^T(q)e_x = \mathbf{0}.$$

can be obtained. This leads in the new coordinates  $w = Q^T(q)e_x$  to a system of  $n$  decoupled equations with the requested damping behaviour:

$$\ddot{w} + 2D_\xi K_{d0}^{1/2} \dot{w} + K_{d0}w = \mathbf{0}. \quad (30)$$

As mentioned before,  $Q(q)$  is here assumed to be quasi-static. Notice that the decoupling can be achieved only in some particular directions, which are given by  $Q(q)$  and hence depend on  $\Lambda(q)$  and  $K_d$ . This is not surprising, since the controller (19) does not provide a decoupling of the mass matrix. Consequently, if the system is excited, oscillations will occur decoupled and with the desired damping behaviour only in those special directions. This is the main limitation of the method.

## VII. EXPERIMENTAL RESULTS

#### A. Nullspace Behaviour

In this experiment the effects of the different nullspace projections from section IV on the Cartesian behaviour are treated. A desired Cartesian impedance behaviour was chosen, which is characterized by the stiffness values in table I and damping values of  $\xi_i = 0.7$ . In this experiment

TABLE I  
COMMANDED VALUES FOR THE DIAGONAL CARTESIAN STIFFNESS MATRIX IN THE FIRST EXPERIMENT.

x	y	z	roll <sup>1</sup>	pitch	yaw
1000	1000	1000	300	300	300
$\frac{N}{m}$	$\frac{N}{m}$	$\frac{N}{m}$	$\frac{Nm}{rad}$	$\frac{Nm}{rad}$	$\frac{Nm}{rad}$

no external forces were present, and therefore, for an ideal nullspace projection, there should be no Cartesian end-effector deviation from the equilibrium point  $x_d$  independently of the manipulator's nullspace motion.

The desired equilibrium point for the nullspace motion was simply chosen as  $q_N = \mathbf{0}$ . The nullspace stiffness and damping matrices were chosen as diagonal matrices  $K_N = k_N I$  and  $D_N = d_N I$ . The initial configuration of the arm can be seen in Fig. 2

In order to generate an oscillating nullspace motion, a negative value was chosen for the damping factor together with a positive value for the stiffness  $k_N$

$$d_N = -0.5k_N^{1/2}, \quad (31)$$

$$k_N = 50 \text{ Nm/rad}. \quad (32)$$

The resulting end-effector motion during the oscillating nullspace motion can then be used for an evaluation of the nullspace projections. In this comparison, only the translational motion of the end-effector shall be used. Then the considered Cartesian error  $\|e_x\|_t$  denotes the

<sup>1</sup>The values for the rotational stiffness were deliberately chosen high, so that the particular representation of orientations has no significant effects on the results, as pointed out in [2], [12].

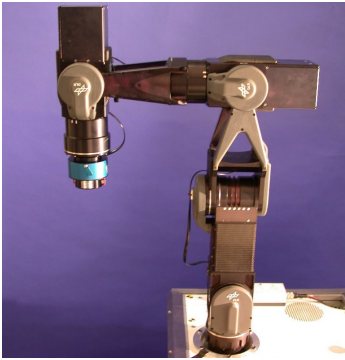


Fig. 2. Initial configuration of the arm for nullspace and damping design experiments.

Euclidean norm of the translational components of  $\mathbf{x} - \mathbf{x}_d$  only. In Fig. 3 these Cartesian errors are shown for the different nullspace projection matrices. Herein the projection matrices were switched online between  $\mathbf{N}_1$ ,  $\mathbf{N}_3$ , and  $\mathbf{N}_2$  during the nullspace oscillation. One can see that the Cartesian errors are considerably larger in case of the static nullspace projection via  $\mathbf{N}_1$ , while the errors with the dynamically consistent projection matrices  $\mathbf{N}_2$  and  $\mathbf{N}_3$  are of similar magnitude.

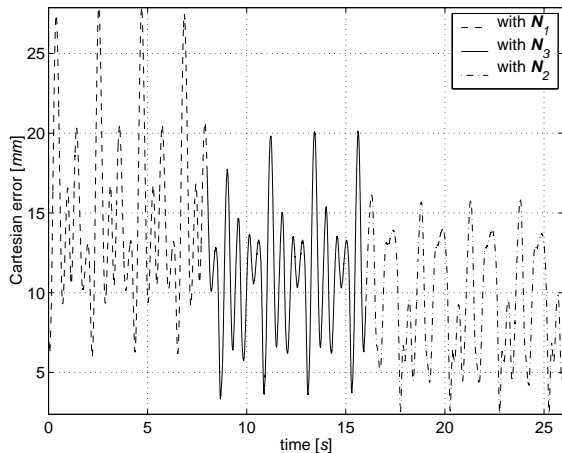


Fig. 3. Cartesian Error  $\|\mathbf{e}_x\|_t$  for the different nullspace projections.

In order to visualize also the nullspace motion, which was present during the generation of Fig. 3, the projection of the joint position deviation  $\mathbf{q} - \mathbf{q}_N$  into the nullspace is given in Fig. 4. While the amplitudes of the oscillations in the nullspace for  $\mathbf{N}_1$  are the lowest (Fig. 4), they result in high Cartesian errors (Fig. 3). One can also see that the period of the oscillation is slightly different for the different nullspace projections. This results from the different weightings of the nullspace stiffness and the damping value by the projection matrices.

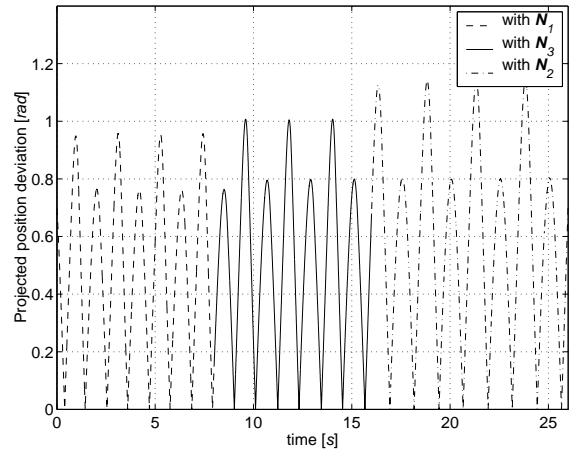


Fig. 4. Projected Joint Error  $\|\mathbf{V}(\mathbf{q})(\mathbf{q} - \mathbf{q}_N)\|_2$  for the different nullspace projections.

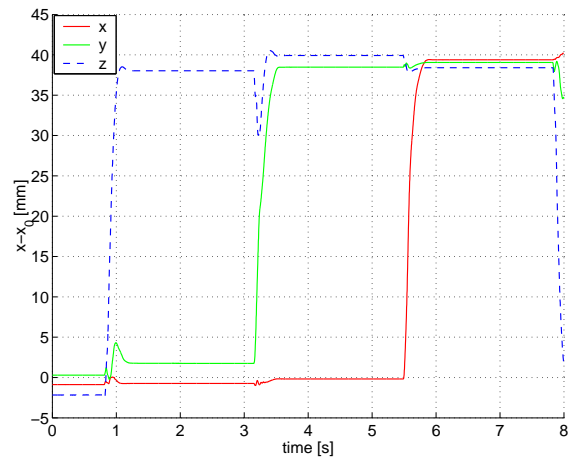


Fig. 5. Position step responses with the factorization damping design for  $\xi_x = \xi_y = \xi_z = 0.7$ .

## B. Damping Design

The effectiveness of the two proposed damping design methods from Sect. VI is evaluated based on step responses which are executed successively in the three translational directions. During the experiment, the desired stiffness values from table II were used.

TABLE II  
COMMANDED VALUES FOR THE DIAGONAL CARTESIAN STIFFNESS MATRIX AND THE NULL-SPACE STIFFNESS.

x	y	z	roll	pitch	yaw	null-space
4000	4000	4000	300	300	300	0.0
$\frac{N}{m}$	$\frac{N}{m}$	$\frac{N}{m}$	$\frac{Nm}{rad}$	$\frac{Nm}{rad}$	$\frac{Nm}{rad}$	$\frac{Nm}{rad}$

The damping values are set to  $\xi_{roll} = \xi_{pitch} = \xi_{yaw} = 0.7$  for the rotations and to  $\xi_n = 0.0$  for the null-space. In Fig. 5, all the step responses are critically damped using the factorization damping design. Since the Cartesian mass

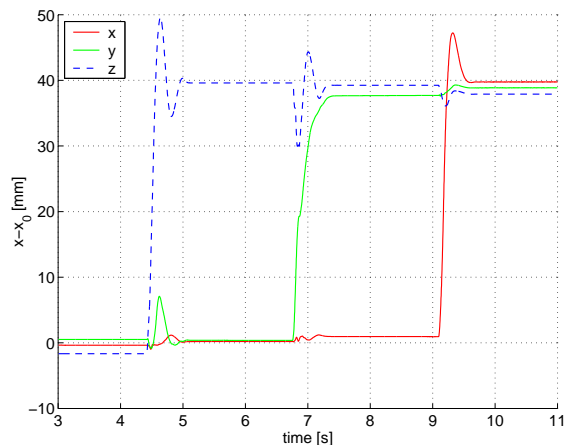


Fig. 6. Position step responses with a starting point  $x_0$ , with the factorization damping design for  $\xi_x = 0.3$ ,  $\xi_y = 1.0$ ,  $\xi_z = 0.3$ .

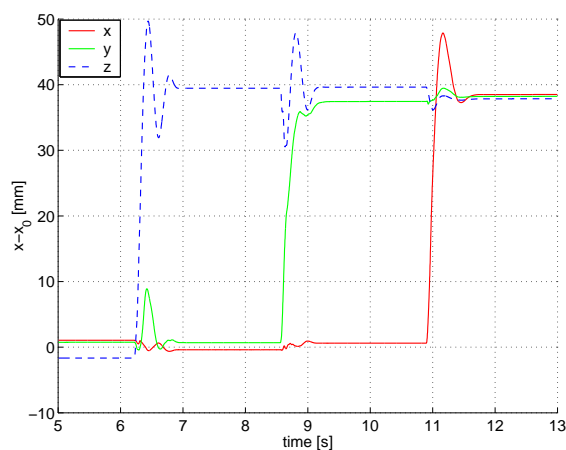


Fig. 7. Position step responses with a starting point  $x_0$ , with the double diagonalization damping design for  $\xi_x = 0.3$ ,  $\xi_y = 1.0$ ,  $\xi_z = 0.3$ .

matrix is not decoupled, it can be seen that a step in one coordinate is exciting also the other directions, but the disturbance is rapidly rejected. The steady-state errors are caused by the lack of perfect compensation of Coulomb friction. Figure 6 and 7 show measurements with the factorization design and the double diagonalization design, respectively, both with the damping set to  $\xi_x = 0.3$ ,  $\xi_y = 1.0$ ,  $\xi_z = 0.3$ . The performance of both methods is similar and corresponds well to the desired one.

## VIII. SUMMARY

In this paper various practically relevant aspects of impedance control for redundant robots have been treated. The actual implementation of the impedance controllers on a flexible joint robot was based on a singular perturbation approach. Three different kinds of nullspace projections for the realization of a nullspace stiffness were described. This aspect has already been treated in detail in the literature and the focus herein lies on the experimental

comparison. Another aspect, which we consider as quite important from a practical point of view, is the design of a suitable damping matrix. This design problem arises when a decoupling of the manipulator's mass behaviour is not possible or not desired. A rather heuristic method as well as a method based on double diagonalization of symmetric positive definite matrices have been presented and experimentally compared.

## ACKNOWLEDGMENT

This work was supported by the German Federal Ministry of Education and Research "BMBF-Leitprojekt MORPHA" number ITL 0902E.

## IX. REFERENCES

- [1] A. Albu-Schäffer and G. Hirzinger. Cartesian impedance control techniques for torque controlled light-weight robots. *IEEE International Conference of Robotics and Automation*, pages 657–663, 2002.
- [2] F. Caccavale, C. Natale, B. Siciliano, and L. Villani. Six-dof impedance control based on angle/axis representations. *IEEE Transactions on Robotics and Automation*, 15(2):289–299, 1999.
- [3] D. Harville. *Matrix Algebra from a Statistician's Perspective*. Springer-Verlag, 1997.
- [4] G. Hirzinger, A. Albu-Schäffer, M. Hähle, I. Schaefer, and N. Sporer. On a new generation of torque controlled light-weight robots. *IEEE International Conference of Robotics and Automation*, pages 3356–3363, 2001.
- [5] N. Hogan. Impedance control: An approach to manipulation, part I - theory, part II - implementation, part III - applications. *Journ. of Dyn. Systems, Measurement and Control*, 107:1–24, 1985.
- [6] O. Khatib. A unified approach for motion and force control of robot manipulators: The operational space formulation. *IEEE Journal of Robotics and Automation*, 3(1):1115–1120, February 1987.
- [7] P. V. Kokotovic, H. K. Khalil, and J. O'Reilly. *Singular Perturbation Methods in Control: Analysis and Design*. Academic Press Inc., 1986.
- [8] A. D. Luca and P. Tomei. *Theory of Robot Control*, chapter Elastic Joints, pages 219–261. Springer-Verlag, Berlin, 1996.
- [9] C. Ott, A. Albu-Schäffer, and G. Hirzinger. Comparison of adaptive and nonadaptive tracking control laws for a flexible joint manipulator. *IEEE Int. Conf. on Intelligent Robots and Systems*, 2002.
- [10] J. Park, W. Chung, and Y. Youm. On dynamical decoupling of kinematically redundant manipulators. *IEEE Int. Conf. on Intelligent Robots and Systems*, 3(1):1495–1500, 1999.
- [11] M. Spong. Modeling and control of elastic joint robots. *IEEE Journal of Robotics and Automation*, RA-3:291–300, 1987.
- [12] S. Stramigioli and H. Bruyninckx. Geometry and screw theory for constrained and unconstrained robot. *Tutorial at ICRA*, 2001.